NeuroImage 201 (2019) 116029

Contents lists available at ScienceDirect

NeuroImage

journal homepage: www.elsevier.com/locate/neuroimage

Mapping critical hubs of receptive and expressive language using MEG: A comparison against fMRI

Vahab Youssofzadeh [a,b,c], Abbas Babajani-Feremi [a,b,d,*]

[a] Department of Pediatrics, University of Tennessee Health Science Center, Memphis, TN, USA
[b] Neuroscience Institute, Le Bonheur Children's Hospital, Memphis, TN, USA
[c] Department of Neurology, Medical College of Wisconsin, Milwaukee, USA
[d] Department of Anatomy and Neurobiology, University of Tennessee Health Science Center, Memphis, TN, USA

ARTICLE INFO

Keywords:
Magnetoencephalography (MEG)
Functional MRI (fMRI)
Language
Whole-brain connectivity
Network hub

ABSTRACT

The complexity of the widespread language network makes it challenging for accurate localization and lateralization. Using large-scale connectivity and graph-theoretical analyses of task-based magnetoencephalography (MEG), we aimed to provide robust representations of receptive and expressive language processes, comparable with spatial profiles of corresponding functional magnetic resonance imaging (fMRI). We examined MEG and fMRI data from 12 healthy young adults (age 20–37 years) completing covert auditory word-recognition task (WRT) and covert auditory verb-generation task (VGT). For MEG language mapping, broadband (3–30 Hz) beamformer sources were estimated, voxel-level connectivity was quantified using phase locking value, and highly connected hubs were characterized using eigenvector centrality graph measure. fMRI data were analyzed using a classic general linear model approach. A laterality index (LI) was computed for 20 language-specific frontotemporal regions for both MEG and fMRI. MEG network analysis showed bilateral and symmetrically distributed hubs within the left and right superior temporal gyrus (STG) during WRT and predominant hubs in left inferior prefrontal gyrus (IFG) during VGT. MEG and fMRI localization maps showed high correlation values within frontotemporal regions during WRT and VGT ($r = 0.63$, 0.74, $q < 0.05$, respectively). Despite good concordance in localization, notable discordances were observed in lateralization between MEG and fMRI. During WRT, MEG favored a left-hemispheric dominance of left STG ($LI = 0.25 \pm 0.22$) whereas fMRI supported a bilateral representation of STG ($LI = 0.08 \pm 0.2$). Laterality of MEG and fMRI during VGT consistently showed a strong asymmetry in left IFG regions (MEG-$LI = 0.45 \pm 0.35$ and fMRI-$LI = 0.46 \pm 0.13$). Our results demonstrate the utility of a large-scale connectivity and graph theoretical analyses for robust identification of language-specific regions. MEG hubs are in great agreement with the literature in revealing with canonical and extra-canonical language sites, thus providing additional support for the underlying topological organization of receptive and expressive language cortices. Discordances in lateralization may emphasize the need for multimodal integration of MEG and fMRI to obtain an excellent predictive value in a heterogeneous healthy population and patients with neurosurgical conditions.

1. Introduction

Mapping and characterization of the underlying structural and functional connectivity patterns of the language network in both healthy and clinical populations is fundamental; It provides important details about how human language processing components are topologically organized to promote cognitive function and how the topology is dynamically reorganized to respond to language abnormalities (Fedorenko and Thompson-Schill, 2014; Hagoort and Indefrey, 2014). Accurately identifying the interaction dynamics of such a functionally complex network is a key challenge in current neuroimaging investigations.

From a classic model of Geschwind (1972, 1970), the neural correlates of the language processing network are linked to activations within distinct cortical regions including anterior portion of the temporal lobe containing primary auditory cortices and adjacent compartments of bilateral superior temporal gyrus (STG) during a receptive process and

* Corresponding author. Department of Pediatrics, University of Tennessee Health Science Center, Neuroscience Institute, Le Bonheur Children's Hospital, 848 Adams Ave, Suite L445A, Memphis, TN, 38103.
E-mail address: ababajan@uthsc.edu (A. Babajani-Feremi).

https://doi.org/10.1016/j.neuroimage.2019.116029
Received 2 March 2019; Received in revised form 8 July 2019; Accepted 16 July 2019
Available online 17 July 2019

posterior convolutions of the left inferior frontal gyrus (IFG) during an expressive process (Binder, 2015; Friederici, 2012; Friederici et al., 2000; Poeppel, 2014; Price, 2000, for review). However, converging evidence from most language studies indicates the involvement of an extensive network of cortical regions with different level of associations (Friederici, 2012; Price, 2012; Pulvermüller and Fadiga, 2010). Receptive processes engage multiple functionally specialized brain regions of the language comprehension including working memory, semantic priming, and cognitive control (Friederici, 2002; Posner et al., 1989; Price et al., 1996). Expressive processes (or language production) requires selection, sequencing, initiation, and motor control (Lidzba et al., 2011; Liljeström et al., 2015a). Such complexity makes accurate localization and lateralization of the language network very challenging for neuroimaging studies.

Lateralization and localization of the language network are routinely investigated using functional magnetic resonance imaging (fMRI) and magnetoencephalography, MEG (Friederici, 2012; Price, 2012). fMRI offers an excellent millimeter spatial resolution but provides an indirect measure of the neural activity with limited spectral dynamics (~0.01–0.12 Hz) and relatively poor temporal resolution, >1s (Byars et al., 2002). In comparison, MEG offers a direct measure of the neural activity with an excellent temporal resolution (<1 msec), moderate spatial precision (mm), and is rich with frequency dynamics up to 100 Hz (Hämäläinen et al., 1993). This makes the MEG favorable for connectivity investigations (i.e. studying dynamics of the brain inter-regional communications) of temporally organized oscillations occurring within milliseconds (Wang et al., 2018). Specifically, MEG is well suited to investigate the dynamics of the language network that is organized via long-range communications and characterized based on their synchrony with other brain circuits (Friederici, 2011; Hagoort and Indefrey, 2014; Turken and Dronkers, 2011).

Connectivity investigations in MEG have disclosed important details about temporal and spectral dynamics of inter-regional interactions within the language network (Doesburg et al., 2012; Kadis et al., 2015; Schoffelen et al., 2017). Kadis et al. (2015) demonstrated frequency-specific connectivity patterns of language verb-generation network in children, together with increased and left lateralized connectivity with age. Schoffelen et al. (2017) characterized reciprocal interactions of the core language sites associated with a sentence/word comprehension language experiment; increased connectivity in alpha and beta bands within fronto-parietal and temporal cortical regions, respectively, were identified as unique characteristics of the language network. Doesburg et al. (2012) demonstrated cross-frequency couplings between short-range gamma (30–50 Hz) synchronization and long-range theta (4–8 Hz) modulation within the left hemisphere expressive language areas, supporting the presence of mechanisms of functional integration in the language network. While previous studies demonstrate the utility of MEG for investigating language network, these studies have focused on specific spectral details that occur in prespecified cortical regions. Additionally, there is no established approach to demonstrate large-scale synchronization patterns of core language regions that accurately reflect hemispheric dominance of expressive and receptive language cortices.

Graph theoretical measures are important tools to handle complex network properties and have been used to characterize the brain networks in healthy individuals and various brain diseases such as Alzheimer, schizophrenia, brain tumors, and epilepsy (He et al., 2010; Stam et al., 2007). Crucially, graph measures reveal important characteristics of topological organization of a network including functional integration that explains the summary statistics of broad connectivity patterns and functional segregation that lead to an identification of specialized regions or local groups (Bullmore and Sporns, 2009; Rubinov and Sporns, 2010). Previous fMRI studies have demonstrated the suitability of the large-scale network analysis in characterizing the network topologies of language processes (Fuertinger et al., 2015; Muller and Meyer, 2014). Similar language studies in MEG are limited. Recently, we conducted a large-scale network connectivity analysis in MEG to characterize and compare core regions of verb generation language network in children and adolescents (Youssofzadeh et al., 2017). The network analysis demonstrated the importance of cortical, subcortical, and cerebellar regions for language development. Consistently, our separate fMRI investigations of a verb-generation task in children led to connectivity clusters within the left IFG, left supramarginal gyrus, and right cerebellar crura as regions being critical for language development (Youssofzadeh et al., 2018b).

Comparisons of MEG and fMRI suggested that both modalities are capable of providing reliable information on lateralization and localization of eloquent (motor, language, and memory) functions (Collinge et al., 2017; Grummich et al., 2006; Liljeström et al., 2015b; Pang et al., 2011; Raghavan et al., 2017; Singh et al., 2002; Vartiainen et al., 2011; Wang et al., 2012). Singh et al. (2002) demonstrated a spatial correlation between cortical desynchronization of MEG source estimates in low-frequency bands (5–15 and 15–25 Hz) and increased hemodynamic fMRI responses of a letter fluency task. Pang et al. (2011), using a time-domain synthetic aperture magnetometry (SAM)-beamformer source analysis, demonstrated a high concordance in localization and lateralization between MEG and fMRI responses during a picture verb-generation task in beta band (15–25 Hz), and verb generation task in low-gamma band (20–35 Hz). Liljeström et al. (2015) investigated large-scale functional connectivity patterns during action/picture-naming task using fMRI and MEG and reported the greatest similarity in functional networks derived from responses below 30 Hz (Liljeström et al., 2015b). They argue that the entire spectral profile of MEG signals should be considered when assessing concordance between MEG neuromagnetic responses and hemodynamic modulations of fMRI.

In the current study, we aimed at developing and validating our proposed MEG pediatric large-scale network mapping approach (Youssofzadeh et al., 2017) to healthy adults' expressive and receptive language networks. Specifically, using MEG and fMRI data collected from healthy young adults during a word-recognition task and a verb-generation task, we sought to demonstrate the suitability of the large-scale MEG network analysis in providing high spatial convergence and consistency in localization and lateralization with hemodynamic modulations of fMRI at individual and group levels. We hypothesized that MEG and fMRI can delineate localization and lateralization of language-specific regions despite differences in the nature of recordings.

2. Material and methods

2.1. Participants

A group of 12 healthy adults participated in this study (5 females, aged 20–37 years, mean ± standard deviation [SD], 27 ± 5.8, see Table 1). Participants were graduate or postgraduate students from the University of Memphis or The University of Tennessee Health Science Center (UTHSC). Participants had no history of neurological insult, speech or language disorder, or learning disability. Written informed consent was obtained from all participants. Study procedures were approved by the Institutional Review Board (IRB) at UTHSC.

Prior to the MEG and fMRI recording sessions, handedness inventory of the participants was determined by self-report as well as by an Edinburgh Handedness Inventory, EHI, test (Oldfield, 1971). EHI greater than 48 were considered as right hemispheric dominance, less than −48 as left hemispheric dominance, and intermediate values as ambidextrous (Oldfield, 1971). Demographic characteristics of participants and their handedness details are summarized in Table 1.

2.2. Stimuli and tasks

Subjects completed two language experiments; a word-recognition "receptive" task (WRT) and a covert auditory verb generation "expressive" task (VGT), in MEG and fMRI. Prior to the recordings, participants

Table 1
Demographic characteristics of participants and their handedness. Edinburgh Handedness Inventory (EHI) greater than 48 were considered as right hemispheric dominance, less than −48 as left hemispheric dominance, and intermediate values as a bilateral. MEG and fMRI laterality examinations of expressive and receptive tasks are also provided. Discordances are specified in orange.

Subj. ID	Age (yr)	Gender	Handedness (EHI)	Laterality (receptive WRT)		Laterality (expressive VGT)	
				fMRI	MEG	fMRI	MEG
1	31	F	100 (R)	-0.15	0.25	0.35	0.65
2	31	F	-50 (L)	0.11	0.21	0.51	-0.61
3	21	F	30 (B)	0.24	0.4	0.63	0.43
4	23	M	-60 (L)	-0.11	-0.21	0.41	0.48
5	23	M	70 (R)	0.40	0.51	0.25	0.49
6	20	F	60 (R)	-0.31	0.31	0.68	0.36
7	36	M	-100 (L)	0.12	0.47	0.42	0.53
8	27	M	30(B)	0.31	0.25	0.35	0.41
9	26	M	50(R)	0.28	0.43	0.34	0.75
10	37	F	70 (R)	0.13	0.27	0.45	0.65
11	29	M	100 (R)	-0.24	-0.15	0.51	0.71
12	21	M	80 (R)	0.21	0.31	0.65	0.64
27±5.8 (Mean±SD)		F=5, M=7	LH=4, RH=6, B=2	0.08±0.2	0.25±0.22	0.46±0.13	0.45±0.35

M: male; F: female; EHI: Edinburgh handedness inventory; LH: left; R: right; B: bilateral; Yr: Year; H: Hemisphere; WRT: word-recognition task; VGT: Verb-generation task

M: male; F: female; EHI: Edinburgh handedness inventory; LH: left; R: right; B: bilateral; Yr: Year; H: Hemisphere; WRT: word-recognition task; VGT: Verb-generation task.

were trained on an overt version of the task to establish sufficient ability and to promote compliance during subsequent acquisition. Schematic presentations of the MEG and fMRI language experiments are shown in Fig. 1. Participants randomly assigned to complete the MEG and fMRI experiments with more than 2 h interval. Due to scanner scheduling conflicts, two subjects completed the MEG and fMRI experiments in two separate days with less than 2 days gap.

2.2.1. MEG language tasks

Participants completed an auditory WRT (Fig. 1). A similar task has been used in previous MEG studies for receptive language examinations (Raghavan et al., 2017; Rezaie et al., 2014). MEG lateralization based on the WRT was demonstrated to be an alternative to the invasive Wada test in patients with epilepsy (Papanicolaou et al., 2004). The stimuli consisted of 40 words designated as "distractors" and 5 words as "targets", read by a native English speaker and presented with a randomly inter-stimulus interval (ISI) of 2–3 s (Fig. 1A). Stimuli were presented in 3 blocks of 45 words, an overall of 135 words. The auditory stimuli were delivered binaurally through two plastic tubes to the participant's outer ear. During the recordings, participants were instructed to lift the index finger of their dominant hand if they recognized each of the five target words.

Participants also performed a covert auditory VGT (Petersen et al., 1988) consisted of 100 stimuli of everyday concrete nouns with scores of 3.0 or higher based on the Paivio Concreteness scale (Paivio et al., 1968). Analogous to WRT, stimuli were auditorily presented, read by a native speaker, and presented with a randomly varied ISI of 2–3 s. Words were chosen from normative databases and standardized language assessments; all were familiar to young adults (e.g., book, dog, airplane). Participants were asked to rapidly think of a verb corresponding to the auditorily presented noun ("AIRPLANE" → "fly"). To minimize artifacts associated with overt speech during the MEG scans, participants were asked to covertly generate the verbs. See Fig. 1B for a schematic presentation of the MEG verb generation paradigm.

2.2.2. fMRI language tasks

Similar to MEG sessions, participants performed the word-recognition and verb-generation tasks in fMRI. Six-minute word-recognition task consisted of twelve 15-s blocks of "word" (10 nouns, 1 target and, 9 distractors) interspersed with 15-s blocks of "control" (9 tones and a bell sound). The 9 pure tones had a frequency from 500 Hz to 2900 Hz with 300 Hz frequency interval. Participants were instructed to lift their index finger if they hear a target (the word, "LITTLE") during the "word" period or a sound of "RINGING BELL" during the "control" period (Fig. 1C). The tones and bell sound in "control" condition were chosen to remove activations in the primary auditory cortex after contrasting this condition to the "word" condition.

Participants performed a 6-min verb-generation task, similar to the task described by (Szaflarski et al., 2012). Stimuli consisted of twelve 15-s blocks of "word" (5 nouns) interspersed with 15-s blocks of "control" (5 tones). Similar to MEG, participants were instructed to rapidly think of an action word that corresponded to the aurally presented nouns during the verb blocks. During control blocks, participants passively listened to five randomly selected pure tones (0.5, 1, 1.5, 2, and 2.5 kHz), and were instructed to perform a bilateral finger tapping, i.e. sequentially touching fingers with the thumb of the same hand, each time they hear a tone. This "control" condition was used to cancel activations in the primary auditory cortex after contrasting with the "verb" condition and for distracting participants from continuing to generate verbs during the control period (Fig. 1D). Regions involved in finger-tapping, motor regions, have minimal overlaps with those known to involve in the verb-generation task (Kemper et al., 2003; Schapiro et al., 2004).

As a difference with fMRI, the control task was not included in the MEG experiment. Instead, prestimulus baseline was used to contrast

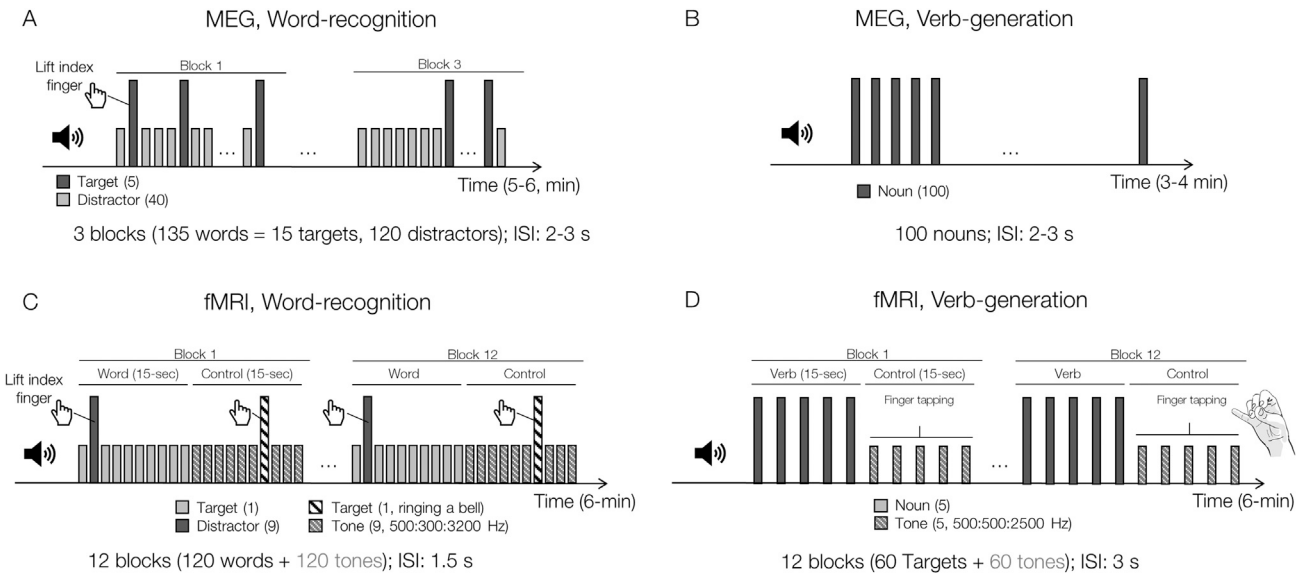

Fig. 1. Language paradigms. (**A**) Word-recognition task used in MEG sessions which consisted of three blocks of words (5 targets and 40 distractors). Stimuli were auditorily presented with a random ISI of 2–3 s. (**B**) Verb-generation task used in MEG sessions consisted of 100 everyday concrete nouns. Stimuli were auditorily presented with a random ISI of 2–3 s. (**C**) Word-recognition task used in fMRI sessions. Stimuli consisted of twelve 15-s blocks of "word" (10 nouns, 1 target, and 9 distractors) interspersed with 15-s blocks of "control" (9 tones and a bell sound). The tones had a frequency range of 500 Hz–2900 Hz with 300 Hz frequency interval. (D) Verb-generation task used in fMRI sessions. Stimuli consisted of twelve 15-s blocks of "word" (5 nouns) interspersed with 15-s blocks of "control" (5 tones).

against post-stimulus task responses. This was supported by the MEG excellent temporal resolution and a covert completion of the tasks (no speech-related effects). Previously, we demonstrated that network hubs corresponding to covert auditory verb generation responses between 400 and 700 ms relative to baseline can successfully reveal the language sites, in children (Youssofzadeh et al., 2017). As an advantage, this design allows a simpler completion of the task and enhanced signal to noise ratio of evoked responses (as more trials are used for averaging). However, including a control data in an MEG experiment is essential for revealing specific aspects of lexicosemantic processes, e.g., differences between real words, pseudowords, consonant letter strings and false fonts (Price et al., 1996; Wang et al., 2012), also for controlling speech-related processes in an overt experiment.

2.3. Data acquisition

Participants underwent MEG and (f)MRI in this study. MEG data were acquired using a whole-head neuromagnetometer array (4-D Neuroimaging, MAGNES WH3600, San Diego, CA) equipped with 248 sensors and housed in a magnetically shielded room with a sampling rate of 1 kHz. The position of the participant's head relative to the sensors was determined using five coils, two of which were anchored to the left and right periauricular points and three on the forehead. The participant's head shape was digitized using a stylus (Polhemus; Colchester, VT) for subsequent localization of activity sources.

Structural and functional MR images were obtained using a 3T Siemens Verio scanner (Siemens AG, Munich, DE) located at Le Bonheur Children's Hospital, Memphis, USA. High-resolution T1 image was acquired with a matrix size of $512 \times 512 \times 192$ and a spatial resolution of 0.5 x 0.5 $\times$ 1 mm. Functional scans were acquired using a *T2**-weighted echo-planar imaging sequence (*TR/TE* = 3000/30 ms; flip angle 90°; voxel size 2.5x2.5 $\times$ 3.5 mm).

2.4. Software note

MEG data were analyzed in FieldTrip toolbox v20180809 (fieldtriptoolbox.org), graph theoretical analysis was carried out using Brain Connectivity Toolbox (sites.google.com/site/bctnet), connectivity and activation patterns were visualized using CONN toolbox ver.17c (web.conn-toolbox.org), and fMRI data were analyzed in SPM12 (www.fil.ion.ucl.ac.uk/spm). All analyses were completed in MATLAB (The Mathworks, Inc.).

2.4.1. MEG data analysis

The proposed framework of large-scale functional network connectivity analysis for language mapping in MEG is shown in Fig. 2. The data processing and analysis steps are described in detail in the following sections.

2.4.1.1. Preprocessing and time-frequency analysis. MEG data were initially epoched from −1 to 2s relative to the onset of stimuli, bandpass filtered from 0.1 to 50 Hz, and baseline corrected using a −500 to 0 ms window. Trials containing artifacts (SQUID jumps, eye-blinks, head movement, muscle) were removed using a semi-automated artifact identification procedure in FieldTrip (fieldtriptoolbox.org/tutorial/automatic_artifact_rejectio). Trials or sensors with a variance that exceeded 3×10^{-24} (fT), kurtosis larger than 15, or z-score larger than 4 were removed. Cardiac artifacts were removed from preprocessed signals using independent component analysis (ICA). On average, five noisy channels, 12 trials, and two ICA components were removed per subject across all participants' data. For task-induced connectivity analysis, MEG responses were analyzed in two intervals of "active" 400–700 ms and "baseline" −400 to −100 ms (Fig. 2A).

To assure the language components were captured, we conducted a time-frequency response (TFR) analysis of sensor-level responses and inspected the presence of event-related desynchronization effects (Kadis et al., 2011; Ressel et al., 2008; Yu et al., 2014). The TFR analysis was conducted using a multitaper time-frequency analysis. Data from all sensors were analyzed in a time and frequency range of −1 to 2 s and 1–50 Hz, respectively. A frequency-dependent sliding time window using a Hanning window length of three cycles ($\Delta T = 3/f$, f is the frequency of interest) was used. Fourier representation was estimated using a spectral smoothing of $\Delta F = 0.8 \times f$. The TFRs were baseline-corrected using 0.3 s before stimulus onset. WRT and VGT time-frequency responses of an individual (S_1) are shown in Fig. 2B. We used these details to support the selection of broadband responses for our subsequent source-level connectivity investigations.

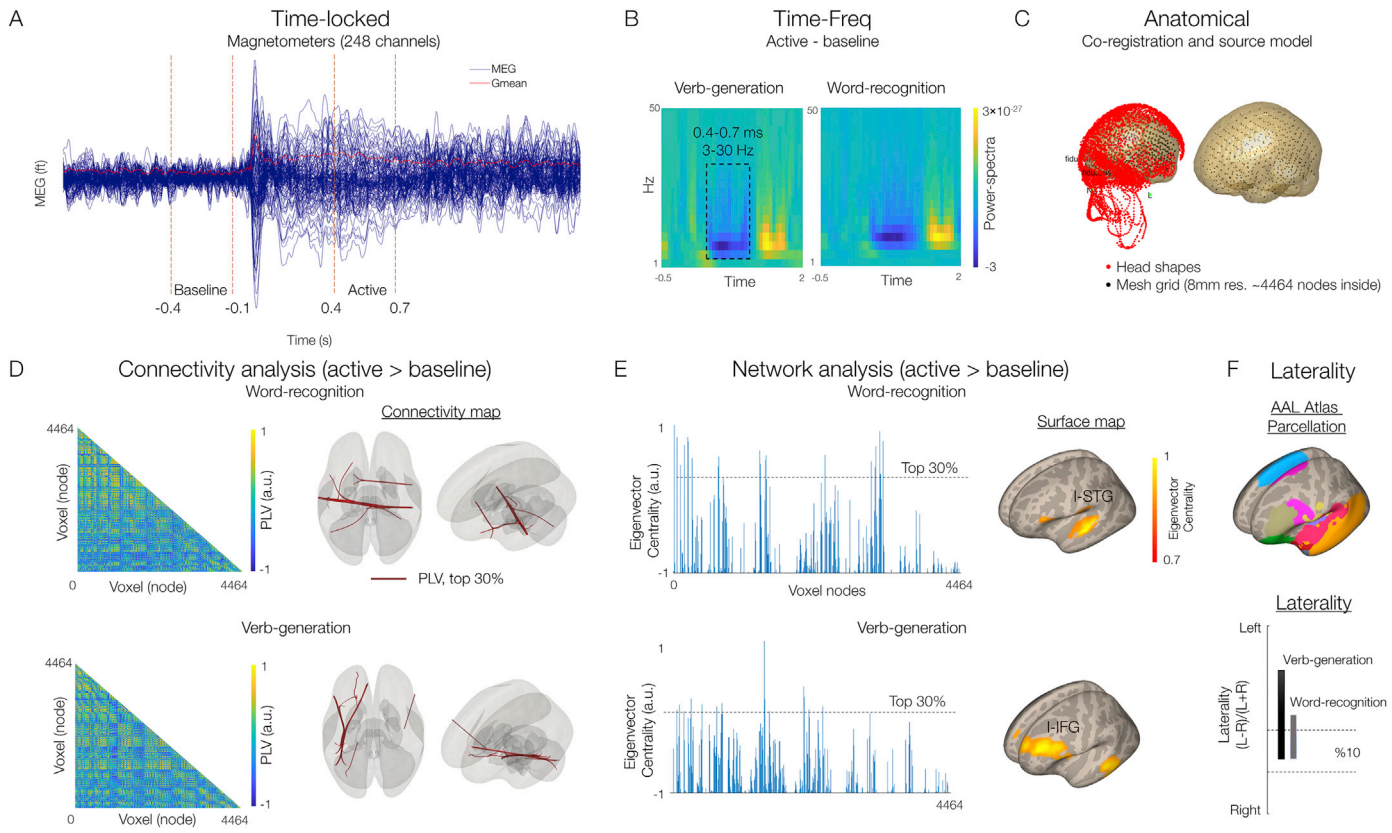

Fig. 2. MEG analysis framework. (**A**) MEG time-locked responses, 248 magnetometers, during word-recognition task (WRT) in a representative subject. Data were preprocessed in the range of 0.1–50 Hz, epoched from −1000 to 2000 ms, and analyzed in an active (400–700 ms) and a baseline (−400 to −100 ms) periods. (**B**) Average time-frequency responses (TFR) during WRT and verb-generation task (VGT). Event-related desynchronization effect was elucidated in a time-frequency range of 400–700 ms and 3–30 Hz, supporting the selection of "active" period. (**C**) Anatomical head model overlaid by a source model. The forward model was estimated using a single-shell model from MRI images of individuals. Source model was constructed using a 3-D grid with a resolution of 8 mm. To account for inter-subject variability in brain macroscopy, grids were warped using a template (SPM12 MNI 152, 8 mm) resulted in 4464 nodes (voxels inside the brain) per individual. (**D**) Source connectivity was quantified using the phase locking value between sources. For representational purposes, a connectivity difference with an arbitrary threshold of top 30% is presented. (**E**) Highly connected hubs were captured through eigenvector centrality (EC). A network difference with an arbitrary threshold of top 30% is presented. (**F**) Language lateralization. AAL atlas was used to parcellate the brain, and 20 cortical parcels at frontotemporal and sensory-motor regions were selected for laterality analysis.

2.4.1.2. MEG beamformer source analysis. MEG data were coregistered to T1-weighted anatomical MRI using common fiducial markers and head shape digitization. T1 images were segmented using SPM8 toolbox to extract brain tissues. A semi-realistic (forward) head model was constructed from segmented scan based on a single-shell description (Nolte, 2003). To account for inter-subject variability in brain macroscopy, atlas-based Montreal Neurological Institute (MNI)-aligned grids in individual head-space were created. As recommended by FieldTrip (fieldtriptoolbox.org/tutorial/sourcemodel), the source model was defined on a regular 3D grid in normalized MNI-space; individual grids were then volumetrically warped to a temple grid (MNI 152 with 8 mm resolution) using a non-linear transformation. To this end, a grid with fixed 4464 grid points inside the brain was obtained, per subject (Fig. 2C).

A lead field matrix and data covariance, necessary for beamforming source inversion, was estimated for all grid points from combined active and baseline conditions, so-called "common filter." The common filter improves source estimation as more data is used for constructing the spatial filters (Haegens et al., 2014; Lindner et al., 2011). Source time-courses were estimated using a time-domain linearly constrained minimum variance (LCMV) beamformer with 1% regularization (Van Veen et al., 1997). LCMV is a time-domain beamforming spatial filter that is optimized to leave untouched the activity originating in the location of interest while suppressing activity from all other areas, assuming that sources are uncorrelated. The low 1% regularization was selected to allow for focal sources during connectivity investigations. A fixed dipole orientation was applied to obtain the strongest orientation that explains most of the source variance to be used during subsequent connectivity investigations.

Of note, beamformer relies on the assumption that no two distinct cortical areas should be perfectly linearly correlated in their activation time series, otherwise very little or no power is recovered (Hillebrand and Barnes, 2005). However, this should be less of a concern for source/connectivity investigations of induced activations as sources are weakly correlated and cortical oscillatory powers do not result in a strong average-evoked activation, e.g. see 400–700 ms responses in Fig. 2A. MEG beamformer has been successfully used for source/connectivity examinations of the language network (Kadis et al., 2011; Schoffelen et al., 2017; Youssofzadeh et al., 2017), and has been validated against fMRI and WADA test (Hirata et al., 2004; Pang et al., 2011).

2.4.1.3. MEG connectivity analysis using phase locking value. Task-induced functional connectivity was estimated using a phase synchrony measure, phase locking value (PLV) (Lachaux et al., 1999). The PLV is defined as, $\mathrm{PLV}(\omega) = \left|\sum e_N^{j\varnothing(\omega))}\right|$ where the phase difference $\varnothing(\omega)$ is derived using Fourier transform of voxel time-series across N trials. The PLV is robust to amplitude fluctuations, sensitive to non-linear interactions (quadratic phase coupling across frequencies) and thus robust to spurious synchronization arising from linear interactions (Darvas et al., 2009). The PLV measure has been successfully tested for

whole-brain network connectivity analysis of both resting-state and task MEG responses (Babajani-Feremi et al., 2018; Schmidt et al., 2014; Youssofzadeh et al., 2017). We computed the average PLV connectivity in the frequency range of 3−30 Hz and time intervals of "active" and "baseline" for all the volumetric grid points (4464 nodes, 8 mm resolution). The broadband frequency was selected as we were interested in capturing the overall connectivity patterns of task-induced responses to quantify the hemispheric dominance of language experiments. Sample PLV connectivity matrices with a top %30 threshold (arbitrary) of WRT and VGT responses from an individual (S_1) are shown in Fig. 2D.

2.4.1.4. Network analysis using eigenvector centrality. Brain hubs associated with highly connected nodes were quantified using *eigenvector centrality* (EC). The EC is a self-referential measure that is computed based on an eigenvector associated with the largest eigenvalue of the adjacency matrix (Fletcher and Wennekers, 2017). The EC is defined as, $C(x) = \frac{1}{\lambda}\sum_{\substack{y\to x \\ w}} w.C(y)$ where $C(x)$ is the centrality for the node x, λ is the largest eigenvalue of the connectivity matrix, and w is the adjacency matrix. Adjacency matrices of active and baseline time intervals were obtained from an arbitrary threshold of 0.7, corresponding to 70% maximum connectivity strength for each subject. The threshold enforced sparsity improves the stability and performance of subsequent graph analyses (see, Youssofzadeh et al., 2018a). For group localization map, EC contrast of active and baseline conditions ($z > 1.96$, approximately 2 standard deviations greater than the mean of individual's responses) were spatially projected (using linear interpolation) onto a surface template in MNI space. Maps corresponding to WRT and VGT responses are shown in Fig. 2E.

Given that our broadband network connectivity analysis may reveal regions that have engagement with lexical so-called N400 and/or post-lexical (decision stage) linguistic effects (Marantz and Pylkka, 2003), we do not make any inferences on specific aspects of the language processing network (e.g., lexical access, semantic processing, and target identification).

2.4.1.5. Atlas parcellation and laterality analysis. A volumetric automated anatomical labeling (AAL) atlas consisting of 116 subdivisions of cortical, subcortical, and cerebellar regions (parcels) was employed to combine and summarize network measures across regions (Tzourio-Mazoyer et al., 2002). For group inferences, network measures with ECs $z > 1.96$ (approximately 2 standard deviations greater than the mean of the individual's responses) were reported as critical hubs.

To characterize hemispheric dominance, we derived a conventional laterality index (LI) from 20 left and right distinct frontotemporal cortical regions: IFG triangular, opercular, and orbital parts; rolandic operculum, supplementary motor area, Heschl's gyrus, superior temporal gyrus, middle temporal gyrus, and temporal pole (superior and middle gyri), as shown in Fig. 2F and 5. Excluding contributions from non-specific language, regions can improve the sensitivity of the laterality analysis (Raghavan et al., 2017). Laterality index was calculated as $LI = (L - R)/(L + R)$, where L and R are the eigenvector centrality values of left and right hemisphere regions, respectively. Following the approach suggested by prior MEG studies (Papanicolaou et al., 2004; Raghavan et al., 2017; Tanaka et al., 2013), LI indices greater than 0.10 were considered left hemispheric dominance, less than −0.10 right hemispheric dominance, and intermediate values as bilateral.

2.4.2. fMRI data analysis

fMRI data were analyzed using a classic general linear model (GLM) approach. Routine pre-processing steps including motion correction, slice-timing correction, spatial normalization, and smoothing (8 mm FWHM Gaussian kernel) were performed. Localization maps were derived from *t*-contrast of "task" against "control" conditions during WRT and VGT for each subject separately. The individual contrast images were used in a second level random effects group analysis. For the group analysis, a voxel-wise significance level of alpha was set to a threshold of $p < 0.05$ corrected for multiple comparisons across the whole brain using family-wise error correction. The fMRI group localization map was compared with that based on MEG.

We note that MEG network approach has been proposed as a language mapping technique, and thus findings are compared with the established

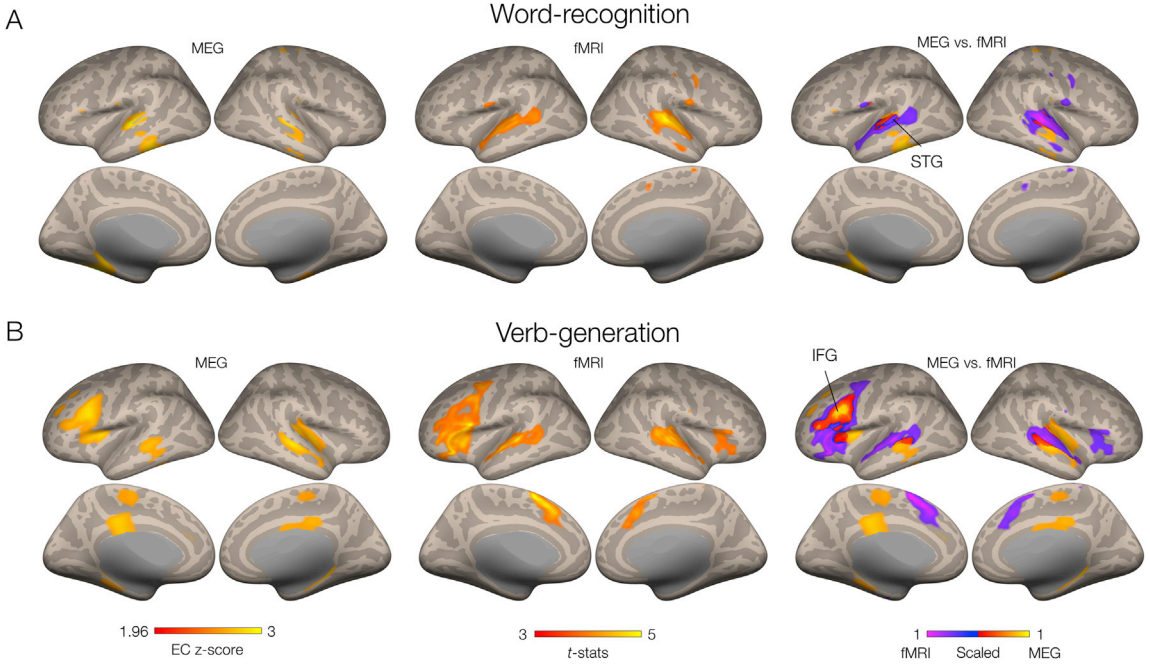

Fig. 3. Group language localization, MEG *vs.* fMRI. (**A**) Network maps captured by eigenvector centrality at the voxel-level during word-recognition task. (**A,** left) MEG results revealed prominent hubs in bilateral superior temporal gyrus (STG) regions, as consistent with GLM-fMRI findings (**A**, middle). As a difference, stronger MEG hubs were identified in the left STG whereas fMRI showed stronger activations on the right STG. (**B**) MEG network analysis of verb-generation task (left) showed prominent hubs in left IFG regions, consistent with fMRI findings (middle). The superimposed MEG and fMRI maps are shown in the right column.

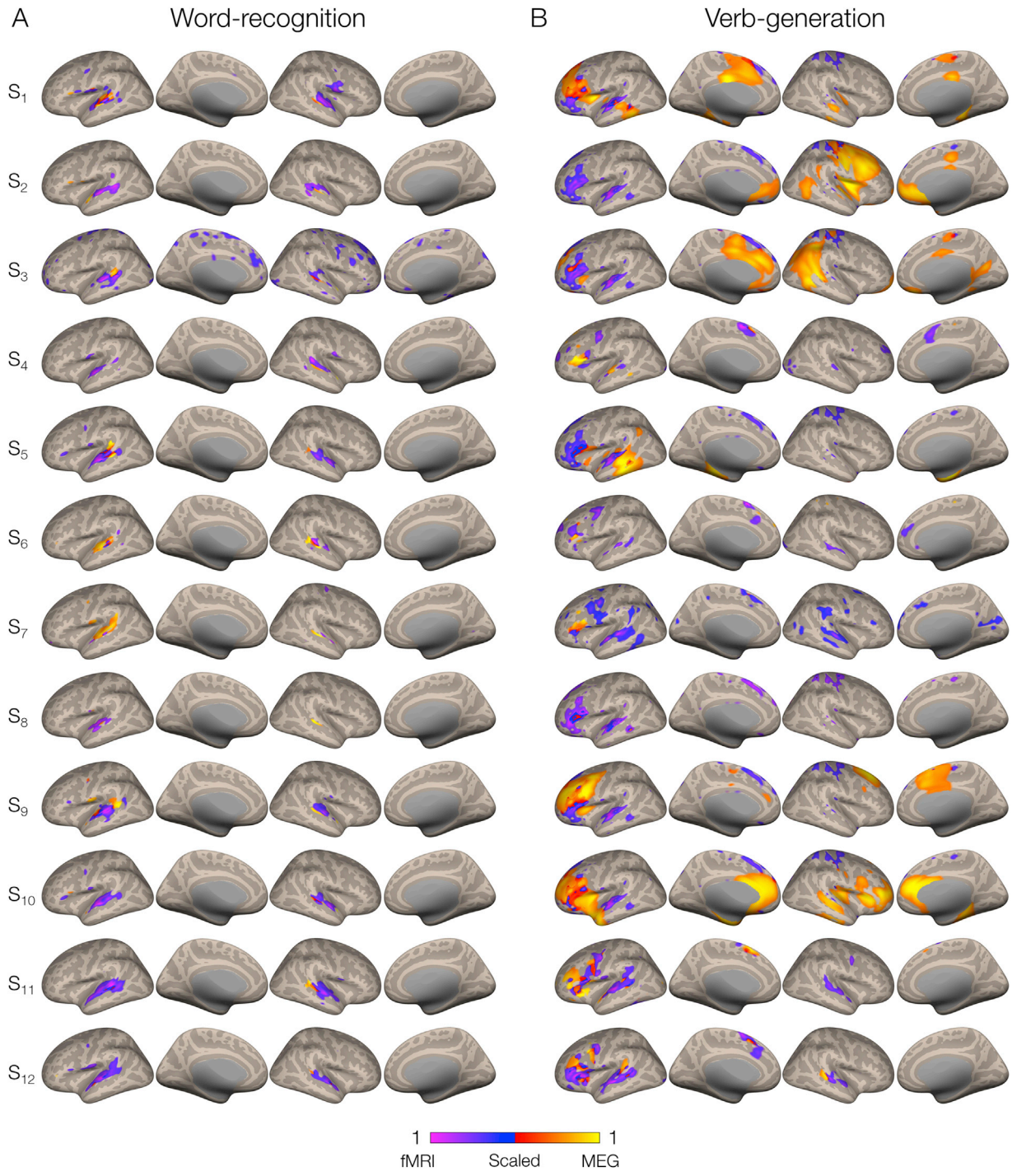

Fig. 4. Language localization of individuals, MEG *vs* fMRI. Overlaid MEG network measures and fMRI *t*-contrast values of individuals during (**A**) word-recognition and (**B**) verb-generation tasks are shown. Results have been scaled in a range of [-1, 1] for presentation purposes. Before rescaling, fMRI and MEG were threshold by *t*-values > 3 and EC z-score > 1.96, respectively.

method of fMRI localization. Investigating differences between MEG and fMRI at the level of connectivity will be considered as a potential extension to our current investigations in the future.

2.4.3. Comparing MEG and fMRI

For comparison purposes, we focused on MEG network hubs ($z > 1.96$) and fMRI contrast values ($t > 3.5$, arbitrary) as we believed those values were likely to be at the core of the language networks. We also conducted a linear bivariate Pearson correlation analysis to assess an overall similarity between MEG network hubs and fMRI *t*-statistics within 20 selected frontotemporal parcels. Correlation *p*-values were corrected for multiple comparisons using a false discovery rate with a critical alpha level of 0.05.

3. Results

In the following sections, handedness and large-scale MEG functional network connectivity patterns associated with WRT and VGT are reported, followed by group-, individual- and ROI-level comparisons between MEG and fMRI localization and lateralization.

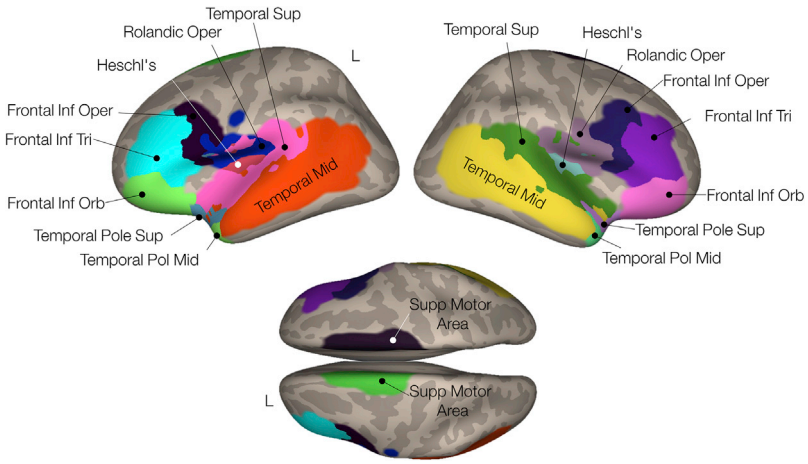

Fig. 5. Language-specific parcels. 20 frontotemporal and sensory-motor cortical regions were selected for language laterality analysis in MEG and fMRI. Random colored areas represent parcellated brain regions according to the AAL anatomical labeling scheme (Tzourio-Mazoyer et al., 2002).

3.1. Handedness and behavioral results

The word recognition task is a very simple task and children with epilepsy and/or cognitive impairment can perform it. Since the subjects of this study were graduate or postgraduate students, their accuracy in identifying the target word in this simple task was 100% in all subjects. We could not monitor accuracy and reaction time of subjects during the verb generation task (VGT) in MEG and fMRI sessions since this task was performed covertly. However, we had a training session before fMRI and MEG data collection, asked subjects to overtly perform the VGT, and observed that they generate appropriate verbs for almost all nouns with a reasonable reaction time.

Handedness examinations based on EHI scores suggested three left-handed, seven right-handed, and two ambidextrous (almost equally left and right) participants (see Table 1). The heterogeneity in handedness allowed us to partially examine the presence of similar mechanisms of language lateralization (e.g. in left-handers) across MEG and fMRI modalities.

3.2. Group, MEG network hubs vs. fMRI t-stats

MEG and fMRI group WRT responses revealed a bilateral and symmetrically distributed pattern of network measures and activations, respectively, within the left and right STG cortical regions (Fig. 3A, left and middle columns), respectively. However, MEG showed stronger network values on the left STG whereas fMRI favored greater effects on the right STG, see **Discussion**. MEG group analysis of VGT responses indicated prominent network values within the left IFG regions (Fig. 3B, left and middle columns). Consistently, fMRI showed asymmetric effects in the left IFG regions. High concordance in localization was found between group MEG and fMRI responses of WRT and VGT (Fig. 3A and B, right column).

3.3. Individuals, MEG network hubs vs. fMRI t-stats

At the individual level, a majority of findings showed high concordances between MEG and fMRI in language sites, e.g. perisylvian cortex during WRT and left IFG during VGT (Fig. 4). An evident discordance was found only in the language localization of one individual. Results from a left-handed female (S_2), showed prominent MEG network values in the right IFG regions during VGT whereas fMRI favored strong effects of the left IFG area. Minor discrepancies (at the level of laterality) were observed in the results of other individuals during WRT. For example, findings from two right-handed females (S_1 and S_6) showed stronger MEG hubs in the left hemisphere while fMRI led to stronger activations in the right-hemispheric homolog.

3.4. ROI analysis: MEG network hubs vs. fMRI t-stats

An ROI analysis was conducted to assess consistency in localization between MEG and fMRI (Fig. 6). MEG results for WRT revealed hubs in bilateral STG cortices, with greater values on the left hemisphere ($EC = 2.59$ in lSTG and $EC = 2.10$ in rSTG). Other hubs were found in bilateral primary auditory cortices, Heschl's gyrus, ($EC = 2.37$ in rHG and $EC = 1.68$ in lHG; right greater than left), and left middle temporal gyrus (MTG, $EC = 1.83$). Consistently, fMRI showed prominent contributions from bilateral STG ($t = 4.00$ in rSTG and $t = 3.28$ in lSTG) and HGs ($t = 2.13$ in rHG and $t = 1.58$ in lHG), with greater activations on the right hemisphere.

MEG results for VGT revealed hubs in the left IFG regions ($EC = 2.8$ in *pars opercularis* and $z = 2.61$ in *pars triangularis*). Other hubs were found in the right HG ($z = 1.60$), right STG ($EC = 1.56$), left supplementary motor area (SMA; $EC = 1.41$), and left MTG ($EC = 1.34$). Consistently, fMRI analysis revealed prominent contributions from the IFG regions ($t = 4.00$ in *pars opercularis* and $t = 3.61$ in *pars triangularis*) and the right STG ($t = 2.6$). A summary contribution of the ROIs is given in Table 2.

MEG network measures and fMRI *t*-statistics significantly correlated within 20 language-specific regions during WRT ($r = 0.63$, $q < 0.05$) and VGT ($r = 0.74$, $q < 0.05$), as in Fig. 6. Expectedly, regions with the highest correlation values were bilateral STG ($r = 0.87$ in rSTG and $r = 0.81$ in lSTG; $q < 0.05$) during WRT and left IFG, *pars opercularis* ($r = 0.89$, $q < 0.05$) and *pars triangularis* ($r = 0.82$, $q < 0.5$) during VGT (Fig. 6A and B, right).

3.5. Laterality analysis (language hemispheric dominance)

Group MEG laterality analysis of WRT favored left-hemispheric dominance, whereas group fMRI indicated a bilateral hemispheric dominance (MEG-LI $= 0.25 \pm 0.22$, fMRI-LI $= 0.08 \pm 0.28$). Laterality of VGT led to high consistency between MEG and fMRI, both modalities indicated strong left-hemispheric dominance (MEG-LI $= 0.45 \pm 0.35$, fMRI-LI $= 0.46 \pm 0.13$), but with lower inter-subject variability, higher stability, by fMRI (MEG-LI-SD $= 0.35 >$ fMRI-LI-SD $= 0.14$). Results are shown in Fig. 7A and B and LI values are reported in Table 1.

4. Discussion

We developed a robust characterization of synchronized oscillatory activity within language-specific brain circuits by combining beamforming source analysis and large-scale network connectivity in MEG. To validate our proposed approach, we conducted two established auditory language experiments, WRT and VGT. We also compared our MEG

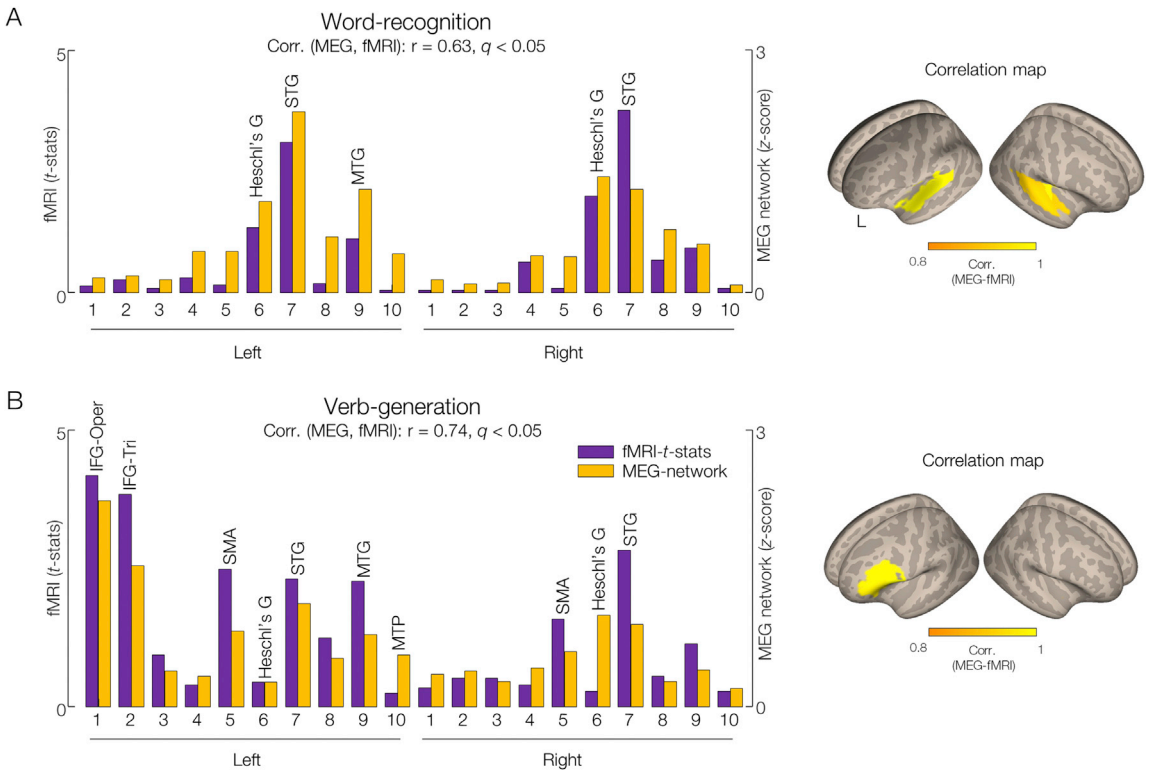

Fig. 6. Group ROI summary**, MEG *vs* fMRI.** MEG eigenvalue centrality and fMRI *t*-stats, during (**A**) word-recognition task and (**B**) verb-generation task in 20 frontotemporal regions. Regions with highest MEG and fMRI correlations (r > 0.8) are shown on the upper-right (word-recognition task) and lower-right (verb-generation task) panels.

Table 2
Summary of group parcellation, MEG-vs-fMRI. Summary of regions of interest (ROIs) detected by MEG network-based parcellated maps and fMRI t-contrast of a group of healthy adults completing receptive word-recognition and expressive verb-generation language tasks.

MEG; Word-recognition				MEG; Verb-generation			
ROI	BA	EC (z-score)	MNI centroid coordinates (x, y, z)	ROI	BA	EC (z-score)	MNI centroid coordinates (x, y, z)
Temporal Sup L	22	2.59	−53, −22, 6	**Frontal Inf Oper L**	44	2.8	−49, 11, 18
Heschl's G R	41/42	2.37	46, −18, 9	**Frontal Inf Tri L**	45	2.61	−46, 29, 13
Temporal Sup R	22	2.10	58, −23, 5	Heschl's R	41/42	1.60	46, −18, 9
Temporal Mid G L	21	1.83	−56, −35, −4	Temporal Sup R	22	1.56	58, −23, 5
Heschl's' G L	41/42	1.68	−42, −20, 9	Supp Motor Area L	6	1.41	−6, 4, 60
				Temporal Mid G L	21	1.34	−56, −35, −4
				Temporal Sup G L	22	1.19	−53, −22, 6
				Supp Motor Area R	6	1.1	6, 4, 60
fMRI; Word-recognition				fMRI; Verb-generation			
ROI	BA	*t*-contrast	MNI centroid coordinates (x, y, z)	ROI	BA	*t*- contrast	MNI centroid coordinates (x, y, z)
Temporal Sup R	22	4	58, −23, 5	**Frontal Inf Oper L**	44	4	−49, 11, 18
Temporal Sup L	22	3.28	−53, −22, 6	**Frontal Inf Tri L**	45	3.6	−46, 29, 13
Heschl's G R	41/42	2.13	46, −18, 9	Supp Motor Area L	6	3.2	−6, 4, 60
Heschl's G L	41/42	1.58	−42, −20, 9	Supp Motor Area R	6	2.6	6, 4, 60
Temporal Mid G L	21	1.51	−56, −35, −4	Temporal Sup R	22	2.6	58, −23, 5
				Temporal Mid G L	21	1.0	−56, −35, −4

BA: Brodmann; ROI: regions of interest; EC: eigenvector centrality; MNI: Montreal Neurological Institute coordinates; L: left hemisphere; R: right hemisphere; Orb: Orbital; Oper: *pars opercularis*; Tri: *pars triangularis*; Sup: Superior; Med: Medial; Inf: Inferior; Supp: Supplementary; EC z-score > 1.96 and fMRI *t*-value > 3.5 are in bold.

findings with results of similar fMRI experiments.

Previous neuroimaging studies have reported that the language comprehension (receptive) and production (expressive) networks are subserved by several distributed regions, including IFG-Broca's and STG-Wernicke's areas (Binder et al., 2009; Friederici, 2011; Hagoort, 2014; Lidzba et al., 2011; Liljeström et al., 2015a; Turken and Dronkers, 2011). Consistently, our MEG network analysis identified hubs within the canonical language regions during word-recognition and verb-generation experiments (Fig. 3, left). In addition, MEG hub analysis revealed involvements of extra-canonical language regions: MTG during the word-recognition and SMA during the verb-generation tasks (Fig. 6 and Table 2). The MTG support the semantic processes of language comprehension (Friederici, 2002; Pallier et al., 2011; Price et al., 1997; Vandenberghe et al., 1996; Wise et al., 1991). Lesions of the MTG lead to semantic deficits and impaired word comprehension; severe aphasia may occur when MTG lesions are accompanied by STG lesions (for review, Binder et al., 2009; Poeppel, 2014). The SMA facilitates spontaneous motor responses to sound during language production (Lima et al., 2016; Tremblay and Small, 2011) and supports silent viewing articulation (Price, 2012). A seed-based functional connectivity study of fMRI

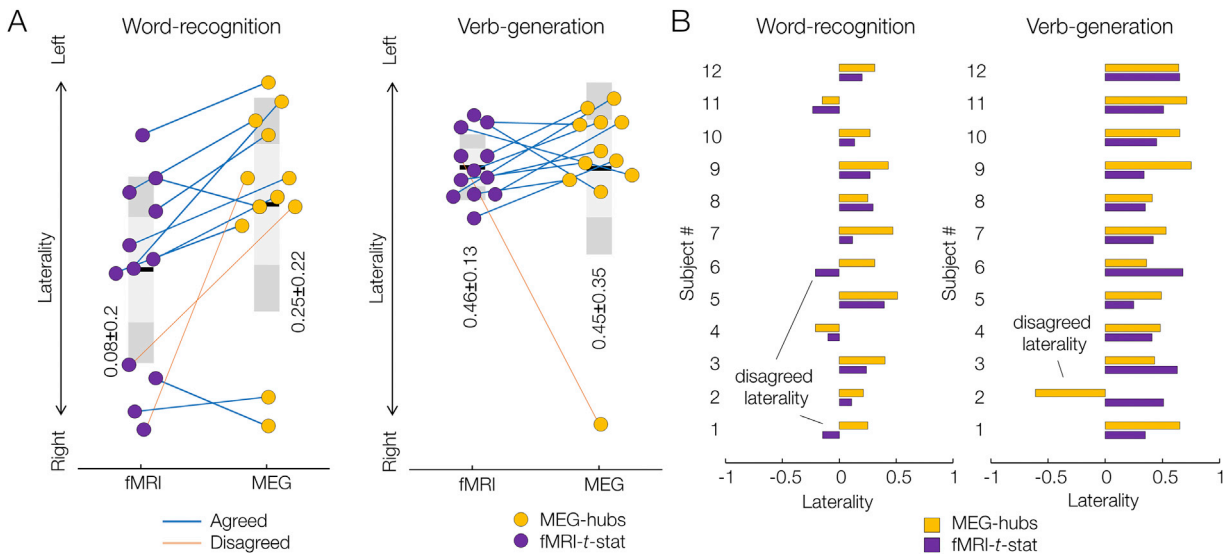

Fig. 7. Laterality analysis, MEG *vs* fMRI. (**A**) Group laterality index MEG hubs vs. fMRI *t*-stats examined in 20 parcels. (**B**) Laterality index of individuals. Positivity and negativity in LI correspond to left- and right-hemispheric dominance, respectively. $|LI|<0.1$ corresponds to symmetric lateralization.

demonstrated significant connectivity between SMA and Broca's area during the task and resting state conditions (Muller and Meyer, 2014). These support the validity of MEG findings and its consistency with the extant literature of the expressive and receptive language.

Our group MEG localization analysis showed high concordances with that of fMRI (Fig. 3, right), in agreement with previous multimodal examinations of the language network (Collinge et al., 2017; Liljeström et al., 2015b; Pang et al., 2011; Raghavan et al., 2017; Singh et al., 2002; Vartiainen et al., 2011; Wang et al., 2012). While MEG and fMRI are interrelated, they may reflect distinct neuronal processes, due to a nonlinear relationship between neuromagnetic and hemodynamic responses in the cortex (Babajani et al., 2005; Babajani and Soltanian-Zadeh, 2006; Singh, 2012). Our multimodal examinations also led to some discrepancies between the two modalities. Specifically, MEG analysis of WRT exhibited a left-hemispheric dominance, in agreement with previous MEG reports on receptive language (Pang et al., 2011; Raghavan et al., 2017; Rezaie et al., 2014). In contrast, fMRI analysis of WRT revealed bilateral activations of left and right STG cortical regions (Fig. 3). Previous studies have argued that this bilateral effect is mainly linked to auditory perceptual processes rather than recognition of specific words (Binder et al., 2008), and this is why temporal lobe activations during a receptive task, e.g. story listening, were not correlated with language dominance from the Wada test (Lehéricy et al., 2000). Hence, the MEG may be considered as a preferred modality for examinations of hemispheric dominance of the auditory receptive language. While our fMRI findings lacked the temporal sensitivity to record brief periods of lateralized receptive language activity within the STG, it reliably lateralized the language in the inferior frontal regions during the VGT. Consistently, fMRI asymmetry of frontal regions during an expressive task, covert sentence repetition, showed strong congruence with Wada test (Lehéricy et al., 2000). MEG network mapping also showed left-lateralized hubs within the left IFG regions but in compare with fMRI had higher interindividual variability (MEG SD = 0.35 > fMRI SD = 0.13, see Fig. 7). One language study argued that MEG may miss long-lasting synchronized events and thus may not encompass the entire extent of the expressive language network (Pang and MacDonald, 2012). While this argument requires further supports by future studies, our results suggest that fMRI is a better modality for examinations of hemispheric dominance of the auditory expressive language. Overall, our findings suggest better reliability of MEG for temporal laterality and fMRI for frontal laterality examinations, emphasizing the need for both modalities for a comprehensive examination of expressive and receptive processes.

Functional specialization at the level of brain networks was suggested to better explain the neuronal architecture of a cognitive function, including language (Bassett et al., 2010; Fedorenko and Thompson-Schill, 2014). Consistent with this theory, our mapping approach explores overall patterns of interdependencies at the level of network community and spatial topography of task-related cortical activations. Crucially, the approach relies on fully data-driven techniques that makes no *a priori* assumptions about the source location, connectivity seeds, and network hubs. Connectivity is derived from broadband (3–30 Hz) sources that contain carrier frequencies of spontaneous electrophysiological activities (Brookes et al., 2011; Hipp et al., 2012). This range is believed to be the key contributor of long-range neuronal communications (Ermentrout and Kopell, 1986; Siegel and Donner, 2010). Broadband examinations have shown a great similarity between MEG and fMRI language networks (Liljeström et al., 2015b). Also, power suppression of broadband rhythms in alpha and beta bands mostly correlate with BOLD-fMRI during task activations (Liljeström et al., 2015b; Singh et al., 2002). All these attest the plausibility our MEG network analysis for language mapping.

MEG source estimates and connectivity can be hindered by unavoidable and inherent phenomena of volume conduction and the instantaneous field spread causing false positive and negative spurious connections (Palva et al., 2018; Wang et al., 2018). To reduce the effect of volume conduction, we analyzed the data at the level of the underlying sources by computing the beamformer filter. Source-space beamformer effectively alleviates the interpretational difficulties introduced by electromagnetic field spread (Gross et al., 2013; Schoffelen and Gross, 2009). We also employed a semi-realistic single shell forward model by Nolte et al. (2004) and computed volume conduction models based on participants' anatomical information to improve the reliability of source estimates. To avoid spurious connections due to averaging effects, we computed the task-induced connectivity (phase synchrony) from source trials. Lastly, we conducted a differential analysis by contrasting the network measures of task and baseline data periods. Benefiting from the concomitant use of fMRI modality for cross-validation we assumed that these strategies effectively cancel out the effects of volume conduction across conditions.

Evaluation of language dominance is a critical step prior to surgery. In the clinical setting, there is no consensus on an optimal methodology for lateralizing language dominance. The dipole fitting has classically been used as a preferred tool for presurgical mapping of the eloquent cortex (Papanicolaou et al., 2004). However, the dipolar methods are

suboptimal for modeling cortical activity of the spatially extensive language network (Raghavan et al., 2017). Laterality estimates based on counting dipoles may be compromised by sensitivity to noise, initialization, and selection of model parameters (Huang et al., 2016). As an alternative, power source mapping based on spatial filtering has been suggested for language mapping in MEG (Doesburg et al., 2015; Hirata et al., 2004; Laaksonen et al., 2012; Piai et al., 2014). However, source localization and power mapping technique alone may not always lead to a full delineation of the patterns of language network, simply because it does not account the interactions among sources. Therefore, we recommend the network mapping approach not only as a complementary but also a key method for language localization and lateralization of the clinical population.

One key challenge of language mapping methods is to determine lateralization with excellent predictive value in a heterogeneous population of neurosurgical candidates (Benjamin et al., 2017). This requires accounting for various factors that may be associated with language laterality including handedness (Friederici et al., 2006; Szaflarski et al., 2012). Handedness was found to be a dependable predictor of hemispheric language dominance in adults (Geschwind and Galaburda, 1985; Kherdr et al., 2002; Knecht et al., 2000). Frequent participation of the right Broca's homolog was found in adults left-handers during a word generation fMRI task (Pujol et al., 1999). This may imply that left-handedness increases the likelihood of right-hemisphere language dominance. However, our multimodal examinations indicated similar patterns of lateralization for most individuals, regardless of their handedness (except S_2, Fig. 4). As future work, a systemic investigation of associations between left-handedness and network-derived language dominance based on large samples can better clarify this argument. Another challenge is to consolidate our understanding of how functional networks interact with their structural substrates. Combining functional connectivity and structural integrity provide this unique insight into the coordination of langue functioning (Ford and Kensinger, 2014; Friederici et al., 2006). Importantly, a functional-structural connectivity analysis can provide a deep understanding of the neuroanatomy and functional integrity of the language network to better explain the heterogeneities of connectivity profiles. Due to lesions or brain injury, language-specific regions may move from their original locations (Grummich et al., 2006). The functional-structural connectivity can also elucidate the consequences of the disruption of white matter pathways, and the contributions of these pathways to functional recovery (Leon-Carrion et al., 2009). Lastly, although word recognition and verb generation tasks are frequently used in language examinations and constitute an essential feature in the comprehension and production of language, they are only one of the multiple dimensions of language. As another future work, including other less restrictive language experiments, e.g. story listening (Lidzba et al., 2011; Schmithorst et al., 2006; Vannest et al., 2009), may help to establish a standard language paradigm optimized for clinical use in pediatric and adults. Uniquely, the story listening task engages the natural syntactic processing in addition to semantic processes (Brennan et al., 2012; Friederici et al., 2003). Importantly, incorporating these details provide a basis for language development and communication (Vigneau et al., 2006).

5. Conclusions

This study was conducted to demonstrate the suitability of large-scale functional network connectivity analysis of MEG responses for lateralizing and localizing brain activity associated with language processing function. By examining the neuronal oscillatory activity of two established auditory word-recognition and verb-generation language tasks in MEG, the proposed large-scale network mapping technique identified critical hubs that support the underlying dynamic topological organization of the healthy adult's language function. Promisingly, localization maps were perfectly matched to the spatial profiles of corresponding fMRI and showed high concordances in laterality across individuals. The framework can be extended to a noninvasive preoperative paradigm to determine language lateralization with excellent predictive value in a heterogeneous population of neurosurgical candidates.

Acknowledgements

This study was funded by Le Bonheur Children's Hospital, the Children's Foundation Research Institute, and the Le Bonheur Associate Board, Memphis, TN. We thank Negar Noorizadeh, Farimah Salami, and Liliya Birg for their contributions in data acquisition.

Appendix A. Supplementary data

Supplementary data to this article can be found online at https://doi.org/10.1016/j.neuroimage.2019.116029.

References

Lachaux, J.P., Rodriguez, E., Martinerie, J., Varela, F.J., 1999. Measuring phase synchrony in brain signals. Hum. Brain Mapp. 8, 194–208. https://doi.org/10.1002/(SICI)1097-0193(1999)8:4<194::AID-HBM4>3.0.CO;2-C.

Babajani, A., Soltanian-Zadeh, H., 2006. Integrated MEG/EEG and fMRI model based on neural masses. IEEE Trans. Biomed. Eng. 53, 1794–1801. https://doi.org/10.1109/TBME.2006.873748.

Babajani, A., Nekooei, M.-H., Soltanian-Zadeh, H., 2005. Integrated MEG and fMRI model: synthesis and analysis. Brain Topogr. 18, 101–113. https://doi.org/10.1007/s10548-005-0279-5.

Babajani-Feremi, A., Noorizadeh, N., Mudigoudar, B., Wheless, J.W., 2018. Predicting seizure outcome of vagus nerve stimulation using MEG-based network topology. NeuroImage Clin 19, 990–999. https://doi.org/10.1016/j.nicl.2018.06.017.

Bassett, D.S., Wymbs, N.F., Porter, M.A., Mucha, P.J., Carlson, J.M., Grafton, S.T., 2010. Dynamic Reconfiguration of Human Brain Networks during Learning, vol. 108. https://doi.org/10.1073/pnas.1018985108.

Benjamin, C.F., Walshaw, P.D., Hale, K., Gaillard, W.D., Baxter, L.C., Berl, M.M., Polczynska, M., Noble, S., Alkawadri, R., Hirsch, L.J., Constable, R.T., Bookheimer, S.Y., 2017. Presurgical language fMRI: mapping of six critical regions. Hum. Brain Mapp. 38, 4239–4255. https://doi.org/10.1002/hbm.23661.

Binder, J.R., 2015. The Wernicke area Modern evidence and a reinterpretation. Neurology 85, 2170–2175. https://doi.org/10.1212/WNL.0000000000002219.

Binder, J.R., Swanson, S.J., Hammeke, T.A., Sabsevitz, D.S., 2008. A comparison of five fMRI protocols for mapping speech comprehension systems. Epilepsia. https://doi.org/10.1111/j.1528-1167.2008.01683.x.

Binder, J.R., Desai, R.H., Graves, W.W., Conant, L.L., 2009. Where is the semantic system? A critical review and meta-analysis of 120 functional neuroimaging studies. Cerebr. Cortex 19, 2767–2796. https://doi.org/10.1093/cercor/bhp055.

Brennan, J., Nir, Y., Hasson, U., Malach, R., Heeger, D.J., Pylkkänen, L., 2012. Syntactic structure building in the anterior temporal lobe during natural story listening. Brain Lang. 120, 163–173. https://doi.org/10.1016/j.bandl.2010.04.002.

Brookes, M.J., Hale, J.R., Zumer, J.M., Stevenson, C.M., Francis, S.T., Barnes, G.R., Owen, J.P., Morris, P.G., Nagarajan, S.S., 2011. Measuring functional connectivity using MEG: methodology and comparison with fcMRI. Neuroimage 56, 1082–1104. https://doi.org/10.1016/j.neuroimage.2011.02.054.

Bullmore, E., Sporns, O., 2009. Complex brain networks: graph theoretical analysis of structural and functional systems. Nat. Rev. Neurosci. 10, 186–198. https://doi.org/10.1038/nrn2575.

Byars, A.W., Holland, S.K., Strawsburg, R.H., Bommer, W., Dunn, R.S., Schmithorst, V.J., Plante, E., 2002. Practical aspects of conducting large-scale functional magnetic resonance imaging studies in children. J. Child Neurol. https://doi.org/10.1177/08830738020170122201.

Collinge, S., Prendergast, G., Mayers, S.T., Marshall, D., Siddell, P., Neilly, E., Ferrie, C.D., Vadlamani, G., Macmullen-Price, J., Warren, D.J., Zaman, A., Chumas, P., Goodden, J., Morrall, M.C.H.J., 2017. Pre-surgical mapping of eloquent cortex for paediatric epilepsy surgery candidates: evidence from a review of advanced functional neuroimaging. Seizure 52, 136–146. https://doi.org/10.1016/j.seizure.2017.09.024.

Darvas, F., Ojemann, J.G., Sorensen, L.B., 2009. Bi-phase locking - a tool for probing non-linear interaction in the human brain. Neuroimage 46, 123–132. https://doi.org/10.1016/j.neuroimage.2009.01.034.

Doesburg, S.M., Vinette, S.A., Cheung, M.J., Pang, E.W., 2012. Theta-modulated gamma-band synchronization among activated regions during a verb generation task. Front. Psychol. 3, 1–11. https://doi.org/10.3389/fpsyg.2012.00195.

Doesburg, S.M., Tingling, K., MacDonald, M.J., Pang, E.W., 2015. Development of network synchronization predicts language abilities. J. Cogn. Neurosci. 28, 55–68. https://doi.org/10.1162/jocn_a_00879.

Ermentrout, G.B., Kopell, N., 1986. Parabolic bursting in an excitable system coupled with a slow oscillation. SIAM J. Appl. Math. 46, 233–253. https://doi.org/10.1137/0146017.

Fedorenko, E., Thompson-Schill, S.L., 2014. Reworking the language network. Trends Cogn. Sci. 18, 120–127. https://doi.org/10.1016/j.tics.2013.12.006.

Fletcher, J.M., Wennekers, T., 2017. From Structure to Activity : Using Centrality Measures to Predict Neuronal Activity, vol. 27. https://doi.org/10.1142/S0129065717500137.

Ford, J.H., Kensinger, E.A., 2014. The relation between structural and functional connectivity depends on age and on task goals. Front. Hum. Neurosci. 8, 1–12. https://doi.org/10.3389/fnhum.2014.00307.
Friederici, A.D., 2002. Towards a neural basis of auditory sentence processing. Trends Cogn. Sci. 6, 78–84. https://doi.org/10.1016/S1364-6613(00)01839-8.
Friederici, A.D., 2011. The brain basis of language processing: from structure to function. Physiol. Rev. 91, 1357–1392. https://doi.org/10.1152/physrev.00006.2011.
Friederici, A.D., 2012. The cortical language circuit: from auditory perception to sentence comprehension. Trends Cogn. Sci. 16, 262–268. https://doi.org/10.1016/j.tics.2012.04.001.
Friederici, A.D., Meyer, M., Cramon, D.Y. von, 2000. auditory language comprehension: an event-related fMRI study on the processing of syntactic and lexical information. Brain Lang. 75, 465–477. https://doi.org/10.1006/brln.2000.2438.
Friederici, A.D., Rüschemeyer, S.A., Hahne, A., Fiebach, C.J., 2003. The role of left inferior frontal and superior temporal cortex in sentence comprehension: localizing syntactic and semantic processes. Cerebr. Cortex. https://doi.org/10.1093/cercor/13.2.170.
Friederici, A.D., Bahlmann, J. r., Heim, S., Schubotz, R.I., Anwander, A., 2006. The brain differentiates human and non-human grammars: functional localization and structural connectivity. Proc. Natl. Acad. Sci. https://doi.org/10.1073/pnas.0509389103.
Fuertinger, S., Horwitz, B., Simonyan, K., 2015. The functional connectome of speech control. PLoS Biol. 13, e1002209 https://doi.org/10.1371/journal.pbio.1002209.
Geschwind, N., 1970. The organization of language and the brain. Science 170, 940–944. https://doi.org/10.1126/science.170.3961.940.
Geschwind, N., 1972. Language and the brain. Sci. Am. 226, 76–83.
Geschwind, N., Galaburda, A.M., 1985. Cerebral lateralization: biological mechanisms, associations, and pathology: III. A hypothesis and a program for research. Arch. Neurol. https://doi.org/10.1001/archneur.1985.04060070024012.
Gross, J., Baillet, S., Barnes, G.R., Henson, R.N., Hillebrand, A., Jensen, O., Jerbi, K., Litvak, V., Maess, B., Oostenveld, R., Parkkonen, L., Taylor, J.R., van Wassenhove, V., Wibral, M., Schoffelen, J.M., 2013. Good practice for conducting and reporting MEG research. Neuroimage 65, 349–363. https://doi.org/10.1016/j.neuroimage.2012.10.001.
Grummich, P., Nimsky, C., Pauli, E., Buchfelder, M., Ganslandt, O., 2006. Combining fMRI and MEG increases the reliability of presurgical language localization: a clinical study on the difference between and congruence of both modalities. Neuroimage 32, 1793–1803. https://doi.org/10.1016/j.neuroimage.2006.05.034.
Haegens, S., Cousijn, H., Wallis, G., Harrison, P.J., Nobre, A.C., 2014. Inter- and intra-individual variability in alpha peak frequency. Neuroimage 92, 46–55. https://doi.org/10.1016/j.neuroimage.2014.01.049.
Hagoort, P., 2014. Nodes and networks in the neural architecture for language: Broca's region and beyond. Curr. Opin. Neurobiol. 28, 136–141. https://doi.org/10.1016/j.conb.2014.07.013.
Hagoort, P., Indefrey, P., 2014. The neurobiology of language beyond single words. Annu. Rev. Neurosci. 37, 347–362. https://doi.org/10.1146/annurev-neuro-071013-013847.
Hämäläinen, M., Hari, R., Ilmoniemi, R.J., 1993. Magnetoencephalography - Theory, Instrumentation, and Applications to Noninvasive Studies of the Working Human Brain. Rev. Mod. Phys. 65, 413–497. https://doi.org/10.1103/RevModPhys.65.413.
He, Y., Evans, A., He, Y., Evans, A., 2010. Graph theoretical modeling of brain connectivity. Curr. Opin. Neurol. 23, 341–350. https://doi.org/10.1097/WCO.0b013e32833aa567.
Hillebrand, A., Barnes, G.R., 2005. Beamformer analysis of MEG data. Int. Rev. Neurobiol. https://doi.org/10.1016/S0074-7742(05)68006-3.
Hipp, J.F., Hawellek, D.J., Corbetta, M., Siegel, M., Engel, A.K., 2012. Large-scale cortical correlation structure of spontaneous oscillatory activity. Nat. Neurosci. 15, 884–890. https://doi.org/10.1038/nn.3101.
Hirata, M., Kato, A., Taniguchi, M., Saitoh, Y., Ninomiya, H., Ihara, A., Kishima, H., Oshino, S., Baba, T., Yorifuji, S., Yoshimine, T., 2004. Determination of language dominance with synthetic aperture magnetometry: comparison with the Wada test. Neuroimage 23, 46–53. https://doi.org/10.1016/j.neuroimage.2004.05.009.
Huang, C.W., Huang, M.X., Ji, Z., Swan, A.R., Angeles, A.M., Song, T., Huang, J.W., Lee, R.R., 2016. High-resolution MEG source imaging approach to accurately localize Broca's area in patients with brain tumor or epilepsy. Clin. Neurophysiol. 127, 2308–2316. https://doi.org/10.1016/j.clinph.2016.02.007.
Kadis, D.S., Pang, E.W., Mills, T., Taylor, M.J., McAndrews, M.P., Smith, M. Lou, 2011. Characterizing the normal developmental trajectory of expressive language lateralization using magnetoencephalography. J. Int. Neuropsychol. Soc. 17, 896–904. https://doi.org/10.1017/S1355617711000932.
Kadis, D.S., Dimitrijevic, A., Toro-Serey, C.A., Smith, M. Lou, Holland, S.K., 2015. Characterizing information flux within the distributed pediatric expressive language network: a core region mapped through fMRI-constrained MEG effective connectivity analyses. Brain Connect. 6, 76–83. https://doi.org/10.1089/brain.2015.0374.
Kemper, S., Herman, R.E., Lian, C.H.T., 2003. The costs of doing two things at once for young and older adults: talking while walking, finger tapping, and ignoring speech or noise. Psychol. Aging. https://doi.org/10.1037/0882-7974.18.2.181.
Kherdr, E.M., Hamed, E., Said, A., Basahi, J., 2002. Handedness and language cerebral lateralization. Eur. J. Appl. Physiol. 87, 469–473. https://doi.org/10.1007/s00421-002-0652-y.
Knecht, S., Drager, B., Deppe, M., Bobe, L., Lohmann, H., Floel, A., Ringelstein, E.B., Henningsen, H., 2000. Handedness and hemispheric language dominance in healthy humans. Brain 123 (Pt 12), 2512–2518. https://doi.org/10.1093/brain/123.12.2512.
Laaksonen, H., Kujala, J., Hultén, A., Liljeström, M., Salmelin, R., 2012. MEG evoked responses and rhythmic activity provide spatiotemporally complementary measures of neural activity in language production. Neuroimage 60, 29–36. https://doi.org/10.1016/j.neuroimage.2011.11.087.
Lehéricy, S., Cohen, L., Bazin, B., Samson, S., Giacomini, E., Rougetet, R., Hertz-Pannier, L., Le Bihan, D., Marsault, C., Baulac, M., 2000. Functional MR evaluation of temporal and frontal language dominance compared with the Wada test. Neurology. https://doi.org/10.1212/WNL.54.8.1625.
Leon-Carrion, J., Martin-Rodriguez, J.F., Damas-Lopez, J., Barroso y Martin, J.M., Dominguez-Morales, M.R., 2009. Delta-alpha ratio correlates with level of recovery after neurorehabilitation in patients with acquired brain injury. Clin. Neurophysiol. 120, 1039–1045. https://doi.org/10.1016/j.clinph.2009.01.021.
Lidzba, K., Schwilling, E., Grodd, W., Krägeloh-Mann, I., Wilke, M., 2011. Language comprehension vs. language production: age effects on fMRI activation. Brain Lang. 119, 6–15. https://doi.org/10.1016/j.bandl.2011.02.003.
Liljeström, M., Kujala, J., Stevenson, C., Salmelin, R., 2015a. Dynamic reconfiguration of the language network preceding onset of speech in picture naming. Hum. Brain Mapp. 36, 1202–1216. https://doi.org/10.1002/hbm.22697.
Liljeström, M., Stevenson, C., Kujala, J., Salmelin, R., 2015b. Task- and stimulus-related cortical networks in language production: exploring similarity of MEG- and fMRI-derived functional connectivity. Neuroimage 120, 75–87. https://doi.org/10.1016/j.neuroimage.2015.07.017.
Lima, C.F., Krishnan, S., Scott, S.K., 2016. Roles of supplementary motor areas in auditory processing and auditory imagery. Trends Neurosci. 39, 527–542. https://doi.org/10.1016/j.tins.2016.06.003.
Lindner, M., Vicente, R., Priesemann, V., Wibral, M., 2011. TRENTOOL: a Matlab open source toolbox to analyse information flow in time series data with transfer entropy. BMC Neurosci. 12, 119. https://doi.org/10.1186/1471-2202-12-119.
Marantz, A., Pylkka, L., 2003. Tracking the Time Course of Word Recognition with MEG, vol. 7, pp. 187–189.
Muller, A.M., Meyer, M., 2014. Language in the brain at rest: new insights from resting state data and graph theoretical analysis. Front. Hum. Neurosci. 8, 228. https://doi.org/10.3389/fnhum.2014.00228.
Nolte, G., 2003. The magnetic lead field theorem in the quasi-static approximation and its use for magnetoencephalography forward calculation in realistic volume conductors. Phys. Med. Biol. 48, 3637–3652. https://doi.org/10.1088/0031-9155/48/22/002.
Nolte, G., Bai, O., Wheaton, L., Mari, Z., Vorbach, S., Hallett, M., 2004. Identifying true brain interaction from EEG data using the imaginary part of coherency. Clin. Neurophysiol. 115, 2292–2307. https://doi.org/10.1016/j.clinph.2004.04.029.
Oldfield, R.C., 1971. The assessment and analysis of handedness: the Edinburgh inventory. Neuropsychologia 9, 97–113. https://doi.org/10.1016/0028-3932(71)90067-4.
Paivio, A., Yuille, J.C., Madigan, S.A., 1968. Concreteness, imagery, and meaningfulness values for 925 nouns. J. Exp. Psychol. https://doi.org/10.1037/h0025327.
Pallier, C., Devauchelle, A.-D., Dehaene, S., 2011. Cortical representation of the constituent structure of sentences. Proc. Natl. Acad. Sci. https://doi.org/10.1073/pnas.1018711108.
Palva, J.M., Wang, S.H., Palva, S., Zhigalov, A., Monto, S., Brookes, M.J., Schoffelen, J.M., Jerbi, K., 2018. Ghost interactions in MEG/EEG source space: a note of caution on inter-areal coupling measures. Neuroimage 173, 632–643. https://doi.org/10.1016/j.neuroimage.2018.02.032.
Pang, E.W., MacDonald, M.J., 2012. An MEG study of the spatiotemporal dynamics of bilingual verb generation. Brain Res. 1467, 56–66. https://doi.org/10.1016/j.brainres.2012.05.054.
Pang, E.W., Wang, F., Malone, M., Kadis, D.S., Donner, E.J., 2011. Localization of Broca's area using verb generation tasks in the MEG: validation against fMRI. Neurosci. Lett. 490, 215–219. https://doi.org/10.1016/j.neulet.2010.12.055.
Papanicolaou, A.C., Simos, P.G., Castillo, E.M., Breier, J.I., Sarkari, S., Pataraia, E., Billingsley, R.L., Buchanan, S., Wheless, J., Maggio, V., Maggio, W.W., 2004. Magnetocephalography: a noninvasive alternative to the Wada procedure. J. Neurosurg. 100, 867–876. https://doi.org/10.3171/jns.2004.100.5.0867.
Petersen, S.E., Fox, P.T., Posner, M.I., Mintun, M., Raichle, M.E., 1988. Positron emission tomographic studies of the cortical anatomy of single-word processing. Nature. https://doi.org/10.1038/331585a0.
Piai, V., Roelofs, A., Jensen, O., Schoffelen, J.M., Bonnefond, M., 2014. Distinct patterns of brain activity characterise lexical activation and competition in spoken word production. PLoS One 9. https://doi.org/10.1371/journal.pone.0088674.
Poeppel, D., 2014. The neuroanatomic and neurophysiological infrastructure for speech and language. Curr. Opin. Neurobiol. 28, 142–149. https://doi.org/10.1016/j.conb.2014.07.005.
Posner, M.I., Sandson, J., Dhawan, M., Shulman, G.L., Unlimited, D., 1989. Is word recognition automatic? A cognitive-anatomical approach. J. Cogn. Neurosci. https://doi.org/10.1162/jocn.1989.1.1.50.
Price, C.J., 2000. The anatomy of language: contributions from functional neuroimaging. J. Anat. 197, 335–59. doi:11117622.
Price, C.J., 2012. A review and synthesis of the first 20years of PET and fMRI studies of heard speech, spoken language and reading. Neuroimage 62, 816–847. https://doi.org/10.1016/j.neuroimage.2012.04.062.
Price, C.J., Wise, R.J.S., Frackowiak, R.S.J., 1996. Demonstrating the implicit processing of visually presented words and pseudowords. Cerebr. Cortex 6, 62–70. https://doi.org/10.1093/cercor/6.1.62.
Price, C.J., Moore, C.J., Humphreys, G.W., Wise, R.J.S., 1997. Segregating semantic from phonological processes during reading. J. Cogn. Neurosci. https://doi.org/10.1162/jocn.1997.9.6.727.
Pujol, J., Deus, J., Losilla, J.M., Capdevila, A., 1999. Cerebral lateralization of language in normal left-handed people studied by functional MRI. Neurology. https://doi.org/10.1212/WNL.52.5.1038.

Pulvermüller, F., Fadiga, L., 2010. Active perception: sensorimotor circuits as a cortical basis for language. Nat. Rev. Neurosci. 11, 351–360. https://doi.org/10.1038/nrn2811.
Raghavan, M., Li, Z., Carlson, C., Anderson, C.T., Stout, J., Sabsevitz, D.S., Swanson, S.J., Binder, J.R., 2017. MEG language lateralization in partial epilepsy using dSPM of auditory event-related fields. Epilepsy Behav. 73, 247–255. https://doi.org/10.1016/j.yebeh.2017.06.002.
Ressel, V., Wilke, M., Lidzba, K., Lutzenberger, W., Krägeloh-Mann, I., 2008. Increases in language lateralization in normal children as observed using magnetoencephalography. Brain Lang. 106, 167–176. https://doi.org/10.1016/j.bandl.2008.01.004.
Rezaie, R., Narayana, S., Schiller, K., Birg, L., Wheless, J.W., Boop, F.A., Papanicolaou, A.C., 2014. Assessment of hemispheric dominance for receptive language in pediatric patients under sedation using magnetoencephalography. Front. Hum. Neurosci. 8, 657. https://doi.org/10.3389/fnhum.2014.00657.
Rubinov, M., Sporns, O., 2010. Complex network measures of brain connectivity: uses and interpretations. Neuroimage 52, 1059–1069. https://doi.org/10.1016/j.neuroimage.2009.10.003.
Schapiro, M.B., Schmithorst, V.J., Wilke, M., Byars, A.W., Strawsburg, R.H., Holland, S.K., 2004. BOLD fMRI signal increases with age in selected brain regions in children. Neuroreport. https://doi.org/10.1097/00001756-200412030-00003.
Schmidt, B.T., Ghuman, A.S., Huppert, T.J., 2014. Whole brain functional connectivity using phase locking measures of resting state magnetoencephalography. Front. Neurosci. 8, 1–15. https://doi.org/10.3389/fnins.2014.00141.
Schmithorst, V.J., Holland, S.K., Plante, E., 2006. Cognitive modules utilized for narrative comprehension in children: a functional magnetic resonance imaging study. Neuroimage 29, 254–266. https://doi.org/10.1016/j.neuroimage.2005.07.020.
Schoffelen, J.-M.M., Gross, J., 2009. Source connectivity analysis with MEG and EEG. Hum. Brain Mapp. 30, 1857–1865. https://doi.org/10.1002/hbm.20745.
Schoffelen, J.-M., Hultén, A., Lam, N., Marquand, A.F., Uddén, J., Hagoort, P., 2017. Frequency-specific directed interactions in the human brain network for language. Proc. Natl. Acad. Sci. https://doi.org/10.1073/pnas.1703155114.
Siegel, M., Donner, T.H., 2010. Linking Band-Limited Cortical Activity to fMRI and Behavior. New York, pp. 1–23.
Singh, K.D., 2012. Which "neural activity" do you mean? fMRI, MEG, oscillations and neurotransmitters. Neuroimage 62, 1121–1130. https://doi.org/10.1016/j.neuroimage.2012.01.028.
Singh, K.D., Barnes, G.R., Hillebrand, A., Forde, E.M.E., Williams, A.L., 2002. Task-related changes in cortical synchronization are spatially coincident with the hemodynamic response. Neuroimage 16, 103–114. https://doi.org/10.1006/nimg.2001.1050.
Stam, C.J., Reijneveld, J.C., Sporns, O., 2007. Graph theoretical analysis of complex networks in the brain. Nonlinear Biomed. Phys. 1, 3. https://doi.org/10.1186/1753-4631-1-3.
Szaflarski, J.P., Rajagopal, A., Altaye, M., Byars, A.W., Jacola, L., Schmithorst, V.J., Schapiro, M.B., Plante, E., Holland, S.K., 2012. Left-handedness and language lateralization in children. Brain Res. 1433, 85–97. https://doi.org/10.1016/j.brainres.2011.11.026.
Tanaka, N., Liu, H., Reinsberger, C., Madsen, J.R., Bourgeois, B.F., Dworetzky, B.A., Hämäläinen, M.S., Stufflebeam, S.M., 2013. Language lateralization represented by spatiotemporal mapping of magnetoencephalography. Am. J. Neuroradiol. https://doi.org/10.3174/ajnr.A3233.
Tremblay, P., Small, S.L., 2011. From language comprehension to action understanding and back again. Cerebr. Cortex 21, 1166–1177. https://doi.org/10.1093/cercor/bhq189.
Turken, A.U., Dronkers, N.F., 2011. The neural architecture of the language comprehension network: converging evidence from lesion and connectivity analyses. Front. Syst. Neurosci. 5, 1. https://doi.org/10.3389/fnsys.2011.00001.
Tzourio-Mazoyer, N., Landeau, B., Papathanassiou, D., Crivello, F., Etard, O., Delcroix, N., Mazoyer, B., Joliot, M., 2002. Automated anatomical labeling of activations in SPM using a macroscopic anatomical parcellation of the MNI MRI single-subject brain. Neuroimage 15, 273–289. https://doi.org/10.1006/nimg.2001.0978.
Vandenberghe, R., Price, C., Wise, R., Josephs, O., Frackowiak, R.S.J., 1996. Functional anatomy of a common semantic system for words and pictures. Nature. https://doi.org/10.1038/383254a0.
Vannest, J.J., Karunanayaka, P.R., Altaye, M., Schmithorst, V.J., Plante, E.M., Eaton, K.J., Rasmussen, J.M., Holland, S.K., 2009. Comparison of fMRI data from passive listening and active-response story processing tasks in children. J. Magn. Reson. Imaging 29, 971–976. https://doi.org/10.1002/jmri.21694.
Vartiainen, J., Liljestrom, M., Koskinen, M., Renvall, H., Salmelin, R., 2011. Functional magnetic resonance imaging blood oxygenation level-dependent signal and magnetoencephalography evoked responses yield different neural functionality in reading. J. Neurosci. 31, 1048–1058. https://doi.org/10.1523/JNEUROSCI.3113-10.2011.
Van Veen, B.D., van Drongelen, W., Yuchtman, M., Suzuki, A., 1997. Localization of brain electrical activity via linearly constrained minimum variance spatial filtering. IEEE Trans. Biomed. Eng. 44, 867–880. https://doi.org/10.1109/10.623056.
Vigneau, M., Beaucousin, V., Herv, P.Y., Duffau, H., Crivello, F., Houdé, O., Mazoyer, B., Tzourio-Mazoyer, N., 2006. Meta-analyzing left hemisphere language areas: phonology, semantics, and sentence processing. Neuroimage 30, 1414–1432. https://doi.org/10.1016/j.neuroimage.2005.11.002.
Wang, Y., Holland, S.K., Vannest, J., 2012. Concordance of MEG and fMRI patterns in adolescents during verb generation. Brain Res. 1447, 79–90. https://doi.org/10.1016/j.brainres.2012.02.001.
Wang, S.H., Lobier, M., Siebenhühner, F., Puoliväli, T., Palva, S., Palva, J.M., 2018. Hyperedge bundling: a practical solution to spurious interactions in MEG/EEG source connectivity analyses. Neuroimage 173, 610–622. https://doi.org/10.1016/j.neuroimage.2018.01.056.
Wise, R., Chollet, F., Hadar, U., Friston, K., Hoffner, E., Frackowiak, R., 1991. Distribution of cortical neural networks involved in word comprehension and word retrieval. Brain. https://doi.org/10.1093/brain/114.4.1803.
Youssofzadeh, V., Williamson, B.J., Kadis, D.S., 2017. Mapping critical language sites in children performing verb generation: whole-brain connectivity and graph theoretical analysis in MEG. Front. Hum. Neurosci. 11, 173. https://doi.org/10.3389/fnhum.2017.00173.
Youssofzadeh, V., Agler, W., Tenney, J.R., Kadis, D.S., 2018a. Whole-brain MEG connectivity-based analyses reveals critical hubs in childhood absence epilepsy. Epilepsy Res. https://doi.org/10.1016/j.eplepsyres.2018.06.001.
Youssofzadeh, V., Vannest, J., Kadis, D.S., 2018b. fMRI connectivity of expressive language in young children and adolescents. Hum. Brain Mapp. 39, 3586–3596. https://doi.org/10.1002/hbm.24196.
Yu, V.Y., Macdonald, M.J., Oh, A., Hua, G.N., Nil, L.F. De, Elizabeth, W., Pang, E.W., 2014. Developmental psychology age-related sex differences in language Lateralization : a magnetoencephalography study in children age-related sex differences in language Lateralization : a magnetoencephalography study in children. Am. Psychol. Assoc. 50, 2276–2284. https://doi.org/10.1037/a0037470.